Polydispersity-Induced Stabilization of the Core−Shell Gyroid

Adam J. Meuler,[†] Christopher J. Ellison,[†] Marc A. Hillmyer,*[,‡] and Frank S. Bates*[,†]

Department of Chemical Engineering and Materials Science and Department of Chemistry, University of Minnesota, Minneapolis, Minnesota 55455

Received May 15, 2008
Revised Manuscript Received July 2, 2008

Most experimental research on block copolymers has focused on "model" macromolecules prepared by living anionic polymerization that contain nearly monodisperse ($M_w/M_n < 1.1$) blocks. Theoreticians have likewise focused on monodisperse block copolymers that approximate those prepared experimentally. Polydispersity effects have become increasingly important, however, as synthetic techniques such as controlled radical polymerization (CRP) have proliferated. While these methods increase the number of monomers easily incorporated into block copolymers, polydispersity indices greater than 1.2 often result.[1,2] Since many block copolymer properties are derived from the underlying mesostructure, understanding the effects of polydispersity on block copolymer phase behavior should aid successful implementation of these materials in advanced technologies. Correspondingly, a number of recent publications have focused on elucidating these effects.[1−16]

The effects of polydispersity have recently been reviewed,[17] and only a short synopsis is provided here. In polydisperse AB diblock and ABA triblock systems, the familiar lamellae, hexagonally packed cylinders, BCC spheres, and gyroid persist but are located over different composition regions depending on the constituent block polydispersities.[8−10,16] Mesostructures with larger mean interfacial curvatures are stabilized by a polydisperse minority block while morphologies with smaller mean interfacial curvatures are favored when the polydisperse block is the major component. This behavior has been attributed to changes in the free energy associated with the entropic elasticity of the polydisperse domains; the longer chains in a collection of polydisperse blocks do not have to stretch as much to fill space, effectively lowering the elastic contribution to the system free energy for the polydisperse ensemble below its monodisperse counterpart.[16] This reduction in elastic free energy is accompanied by an increase in domain spacing in block copolymer melts[3−5,9,10,15] and results in an increase in the height of end-grafted polymer brushes.[18] It also can drive morphological transitions in block copolymer melts because there is a tendency to curve an interface toward the "softer" polydisperse block so that chains in the opposing domain may relax.[8−10,16] Polydispersity-driven macrophase separation has been reported in both homopolymer/polydisperse diblock[2] and multicomponent diblock/diblock[3−5] blends and is predicted to occur for some polydisperse diblock copolymers with continuous molecular weight distributions.[16]

While research thus far has focused on understanding polydispersity effects, Leibler has noted that "... foreseeing how to benefit from polydispersity and some controlled molecular disorder..." will facilitate the development of designer materials.[19] In this work, polydispersity is judiciously introduced into the poly(ethylene oxide) (PEO) block of poly(isoprene-*b*-styrene-*b*-ethylene oxide) (ISO) triblock terpolymers to stabilize the core−shell gyroid (CSG) network mesostructure at a composition where it is not stable for the monodisperse analogue. Multiply continuous network morphologies like CSG can have superior mechanical properties (compared to their 1-D and 2-D counterparts)[20,21] and could find utility in technologies such as catalysis,[22] photonic materials,[23,24] and separations.[25] The stabilization of CSG illustrates that polydispersity should be viewed as a tool for tuning phase behavior.[19,26]

A hydroxyl-terminated IS diblock (IS-OH) was synthesized by sequential anionic polymerization in cyclohexane using *sec*-butyllithium as the initiator. The living chains were end-capped with ethylene oxide and terminated with degassed methanol.[27] Five ethylene oxide polymerizations were initiated from the isolated IS-OH diblock using an established protocol.[28] Room temperature size exclusion chromatography (SEC) experiments were performed using a differential refractometer and tetrahydrofuran as the mobile phase. Data were calibrated with polyisoprene (PI) (a PI aliquot) or polystyrene (PS) (for PS, IS, and ISO) standards to determine M_n of the first PI block and M_w/M_n for all polymers (PS was measured following degradation of the PI in the IS diblock via ozonolysis in toluene solution at −78 °C). The composition and overall M_n of each ISO triblock were determined using ^{1}H NMR spectroscopy and the measured M_n of the PI block. The uncertainties in M_n and f_i are, based upon the reproducibility of the measurements, ±5% and ±0.01, respectively.

Synchrotron small-angle X-ray scattering (SAXS) experiments were conducted using the instrumentation maintained by the Dupont−Northwestern−Dow Collaborative Access Team (DND-CAT) at the Advanced Photon Source at Argonne National Laboratory. Dynamic mechanical spectroscopy (DMS) experiments were conducted using a Rheometrics Scientific ARES rheometer. Order−disorder transition temperatures (T_{ODT}'s) produced a sharp drop in the dynamic elastic modulus upon heating the polymers at 1 °C/min[29] and were consistent with characteristic changes in SAXS patterns. All SAXS and DMS samples were heated 10 °C above T_{ODT} (or to 250 °C) before data were collected to erase the effects of thermal history. The molecular characteristics of the IS diblock, five ISO triblocks, and an ISO blend are summarized in Table 1.

Representative SAXS data obtained from four of the ISO triblocks are presented in Figure 1. The Bragg peaks for ISO(0.05) and ISO(0.33) are indexed to a lamellar mesostructure; the absence of the 002 peak in ISO(0.05) is consistent with a structure factor extinction for symmetric two-domain lamellae (LAM_2).[31] The SAXS data for ISO(0.44) (not shown) also index to lamellae. The LAM_2 and three-domain lamellar (LAM_3) morphologies were previously identified in higher molecular weight ISO triblocks with comparable compositions.[27,31−33] The SAXS data for ISO(0.21) are definitively indexed to the CSG. The SAXS data for ISO(0.28) contain Bragg peaks characteristic of both CSG (marked by ◆ in Figure 1) and the orthorhombic *Fddd* network (herein called O^{70}, where "O" indicates an orthorhombic unit cell and "70" refers to the number of the space group in the crystallographic tables[34]). The *hkl* labels in Figure 1 mark the first seven reflections allowed by the O^{70} space group symmetry.[34] While it is possible that

* To whom correspondence should be addressed. E-mail: hillmyer@umn.edu, bates@cems.umn.edu.
[†] Department of Chemical Engineering and Materials Science.
[‡] Department of Chemistry.

10.1021/ma8010894 CCC: $40.75
Published on Web 08/16/2008

Table 1. ISO Characterization Data

sample[a]	N_I[b]	N_S[b]	N_O[b]	f_O[c]	M_n (kDa)	M_w/M_n	lattice dimensions[d] (nm)	phase[e]	T_{ODT}[f] (°C)
IS	81	84	0	0	10.6	1.08	12.5 (80 °C)	DIS	
ISO(0.05)	81	84	9	0.05	11.3	1.10	13.9 (80 °C)	LAM_2	88
ISO(0.21)	81	84	44	0.21	13.9	1.10	44.0	CSG	242
ISO(0.28)	81	84	64	0.28	15.4	1.12	0.280, 0.578, 77.3	O^{70}/CSG[g]	>250
ISO(0.33)	81	84	81	0.33	16.7	1.14	20.4	LAM_3	>250
ISO(0.44)	81	84	130	0.44	20.4	1.19	23.0	LAM_3	>250
ISO(0.33, 1.30)	81	84	81	0.33	16.7	1.30[h]	53.6	CSG	>250

[a] M_w/M_n values for the PI and PS blocks are 1.10 and 1.06, respectively; these quantities were measured using SEC calibrated with PI and PS standards. [b] Number-average degrees of polymerization (N_i) based on a segment reference volume of 118 Å^3 and calculated using published density values at 140 °C ($\rho_I = 0.830$, $\rho_S = 0.969$, $\rho_O = 1.064$ g/cm^3).[30] [c] Volume fractions calculated from the provided N values. [d] Lattice dimensions are obtained from SAXS data and are reported at 120 °C unless otherwise noted in parentheses. The lattice dimensions listed for O^{70} correspond to *a*/*c*, *b*/*c*, and *c* while the value listed for IS corresponds to the length scale associated with the first peak in the scattering data. [e] Morphologies were identified using SAXS data at 120 °C unless otherwise noted in parentheses. [f] Measured using DMS. [g] Bragg peaks characteristic of both O^{70} and CSG were identified at 120 °C; the intensities of the O^{70} peaks were higher so the listed lattice parameters are for O^{70}. [h] M_w/M_n value for the PEO block, calculated by assuming the PEO chains in the four neat ISO triblocks are monodisperse.

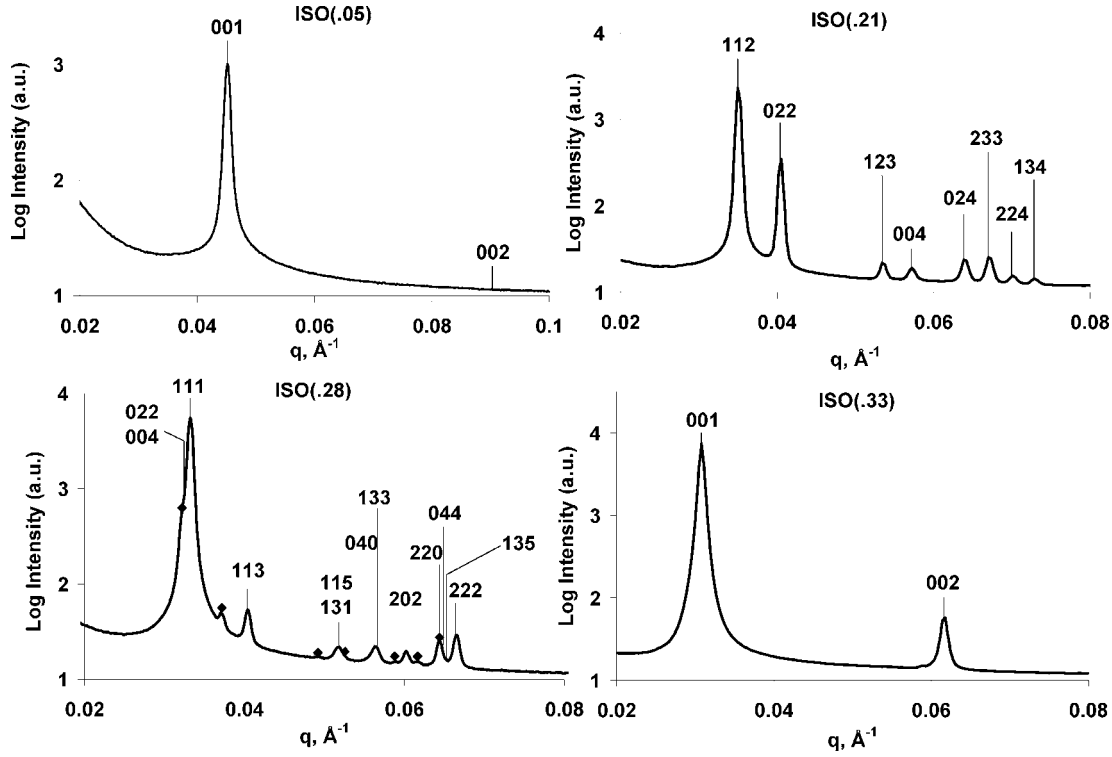

Figure 1. Synchrotron SAXS data acquired at 120 °C (80 °C for ISO(0.05)). All samples were annealed at 250 °C (at 100 °C for ISO(0.05)) for 5 min and then at the target temperature for 5 min before data were collected. The data for ISO(0.05) and ISO(0.33) are indexed to a lamellar morphology; the absence of the 002 peak in ISO(0.05) is consistent with a structure factor extinctions for symmetric LAM_2.[31] The Bragg peaks for ISO(0.21) are indexed to CSG. The peaks in the diffraction pattern for ISO(0.28) are indexed to both O^{70} (*hkl* labels mark the first seven reflections allowed by the O^{70} space group symmetry[34]) and CSG (marked by ◆); this coexistence is likely metastable.

ISO(0.28) has fractionated into CSG and O^{70},[16] the coexistence is likely metastable, as the sample was only annealed for 5 min. Both ISO(0.21) and ISO(0.28) adopted morphologies that were not identified at comparable compositions in the previous higher molecular weight ISO studies (M_n of parent IS diblock = 13.6 kg/mol),[27,31,32] suggesting that phase behavior depends on the segregation strength of the materials.

Tyler, Morse, and co-workers calculated the free energies of a number of morphological candidates for ISO triblocks using self-consistent field theory (SCFT) and identified O^{70} as an equilibrium morphology along the $f_I \approx f_S$ isopleth ($0.19 < f_O < 0.25$).[35,36] They used a pseudospectral method and varied the composition while keeping the overall N (with 118 Å^3 reference volume) of the ISO triblock constant at 250, a chain length relevant to the experiments of Bailey, Epps, Cochran, Bates, and co-workers.[27,31,32] We used the same SCFT code, with the identical χ parameters and statistical segment lengths (b) previously employed,[35,36] but varied molecular weight to mimic our experiments. N of the IS diblock was kept constant at our experimental value ($N_I = 81$ and $N_S = 84$), and the length of the PEO chain was adjusted, mirroring the synthetic methodology used to prepare the ISO triblocks listed in Table 1. The free energies of five morphological candidates were computed: lamellae (LAM), CSG, O^{70}, PEO cylinders packed hexagonally in an IS matrix (HEX_O), and PI cylinders packed hexagonally in an SO matrix (HEX_I). The free energies of these morphologies, relative to that of LAM and normalized by k_BT, are presented in Figure 2. The free energy curve for O^{70} terminates at $f_O = 0.11$ and $f_O = 0.32$ due to technical issues that prevent the location of SCFT solutions (see ref 36 for more details). As f_O increases, the predicted phase sequence is LAM → O^{70} → LAM, the same sequence predicted by Tyler et al.[36] While Tyler et al.'s SCFT calculations do predict the sequence of equilibrium morphologies identified in the experimental ISO reports,[31,32] there are quantitative discrepancies in the exact positions of the phase boundaries. It is therefore not surprising that our SCFT

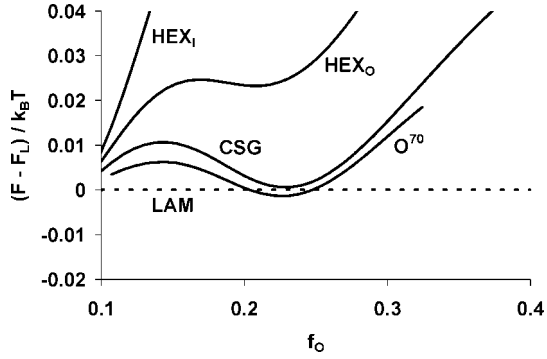

Figure 2. SCFT free energies of four mesostructural candidates, relative to LAM and normalized by k_BT, along the $f_I = 0.49$, $f_S = 0.51$ isopleth. The predicted stable morphologies are, from left to right, LAM, O^{70}, and LAM. The free energy curve for O^{70} terminates at $f_O = 0.11$ and $f_O = 0.32$ due to a previously reported technical issue that prevents the identification of SCFT solutions (see ref 36 for more details).

calculations do not identify CSG as an equilibrium microstructure along the $f_I \approx f_S$ isopleth, especially considering that the calculated free energy differences between CSG, LAM, and O^{70} are less than 0.01 k_BT for $0.20 < f_O < 0.25$. Given these comparable free energies of CSG and O^{70}, the uncertainty in composition measurements, and the differences in segregation strength, it is also not surprising that we identified CSG as the presumably equilibrium mesostructure for sample ISO(0.21) while O^{70} was identified in a higher molecular weight polymer with a comparable composition.[31,32] Miao and Wickham have suggested that composition fluctuations can destabilize O^{70} in AB diblock copolymers, although their predictions only apply to materials near the order−disorder transition.[37]

In a previous report,[14] we interrogated the phase behavior of ISO triblocks with increased polydispersity in the PS block ($M_w/M_n = 1.31$) and identified lamellae in the network "window" ($f_I \approx f_S$ isopleth, $0.13 < f_O < 0.24$). PS polydispersity drove a transition from a network mesostructure (O^{70} or CSG) to LAM. One could be tempted, on the basis of this result, to consider high polydispersity to be detrimental to the formation of multiply continuous network structures. However, this assessment considers polydispersity in just one of the blocks. We anticipate that polydispersity can be used to drive the opposite morphological transition (i.e., from LAM to a network morphology). Previous studies have demonstrated that domain interfaces tend to curve toward the polydisperse block.[8−10,16] We hypothesize that broadening the molecular weight distribution (MWD) of the terminal PEO blocks of an ISO sample with a LAM_3 mesostructure will drive the interface to curve toward the PEO domains and stabilize a network morphology. In the work described here, polydispersity was introduced into the PEO blocks by multicomponent blending.[3−5,38] ISO(0.05), ISO(0.21), ISO(0.28), and ISO(0.44) were solution blended by dissolution in and freeze-drying from benzene; the mass fractions of the components in blend ISO(0.33, 1.30) are 0.079, 0.161, 0.247, and 0.513, respectively. Since all of the ISO triblocks were synthesized from the same parent IS diblock, only the MWD of the PEO block changes upon blending. $M_w/M_n = 1.30$ was calculated for the PEO domains by assuming the neat ISO triblocks contained perfectly monodisperse PEO chains.

Blend ISO(0.33, 1.30) has a composition and overall M_n identical to those of triblock ISO(0.33), a sample that formed the LAM_3 morphology. Any differences in the phase behavior of these two samples must be driven by the differences in the distributions of the PEO chain lengths. Synchrotron SAXS data for blend ISO(0.33, 1.30) are provided in Figure 3; the peaks

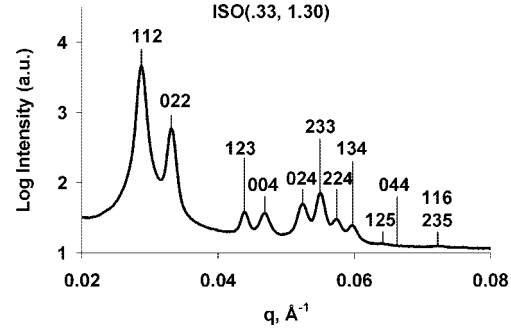

Figure 3. Synchrotron SAXS data acquired at 120 °C for blend ISO(0.33, 1.30). The blend was annealed at 250 °C for 5 min before a 5 min anneal at 120 °C. The Bragg peaks are indexed to the CSG mesostructure.

Table 2. Differences in Free Energy Components ($F_{CSG} - F_{LAM}$) and Relative Domain Spacings of the LAM_3 and CSG Morphologies for ISO Samples with $f_O = 0.33$ (All Free Energies Are Normalized by k_BT)

PEO PDI	$F_{CSG} - F_{LAM}$[a]	ΔF_I[b]	ΔF_O[b]	ΔF_{IS}[c]	ΔF_{SO}[c]	ΔF_{IO}[c]	ΔF_{excess}[d]	d^*_{CSG}/d^*_{LAM}[e]
1.00	0.026	−0.033	0.079	0.040	−0.040	0.030	−0.050	1.039
1.30	−0.017	−0.033	0.051	0.029	−0.045	0.020	−0.039	1.060

[a] Differences in the overall Helmholtz free energy. [b] Differences in the free energy associated with the conformational entropies of the PI and PEO blocks. [c] Differences in the interaction energies of IS, SO, and IO monomer pairs. [d] Differences in the excess free energy, a quantity that includes the entropic free energy associated with stretching the PS block and the entropic free energy associated with the localization of chain junction points. [e] Ratio of the length scales associated with the principal scattering vector ($d^* = 2\pi/q^*$).

are indexed to the CSG mesostructure. Selective broadening of the PEO MWD has driven a morphological transition from LAM_3 (sample ISO(0.33)) to CSG (blend ISO(0.33, 1.30)).

SCFT calculations were performed to understand the physics of the polydispersity-driven LAM_3 to CSG transition. The inputs for the SCFT calculations were models of the ISO triblock terpolymers in blend ISO(0.33, 1.30): monodisperse ISO(0.05), ISO(0.21), ISO(0.28), and ISO(0.44) triblocks with N_i values listed in Table 1 and with the relative masses listed previously. Five morphological candidates were considered: LAM, CSG, O^{70}, HEX_O, and HEX_I. Since there was no experimental evidence of macrophase separation (e.g., no coexistence of morphologies evident in the high-resolution SAXS data in Figure 3), fractionation of the polymers into two different mesostructures[16] was not considered. For the blend, the CSG has the lowest overall free energy, a result that corroborates the SAXS data presented in Figure 3. To understand why increasing PEO polydispersity stabilizes CSG, the components of the free energies of CSG and LAM for neat ISO(0.33) and blend ISO(0.33, 1.30) were examined; the differences in these values are provided in Table 2 for PEO PDI = 1 and PEO PDI = 1.30.

We believe the thermodynamic driving force for the polydispersity-induced stabilization of the CSG is related to the magnitudes of chain stretching summed over the distribution of chain lengths. The exact overall contribution to the system free energy will be sensitive to the chain length distribution function of the PEO (and PS and PI) chains.[13] The increased polydispersity in the PEO block alleviates the entropic penalty (ΔF_O) incurred by the PEO chains as they stretch to accommodate the CSG mesostructure; ΔF_O declines from 0.078 to 0.051 as the PEO PDI is increased from 1 to 1.30 (Table 2). Presumably the longer PEO chains occupy the center of the domain while the shorter chains adopt relaxed conformations

near the domain interface or mix with the PI or PS domains.[6−9,15] In addition to the change in ΔF_O, the increased polydispersity of the PEO block reduces the enthalpic penalty ($\Delta F_{IS} + \Delta F_{SO} + \Delta F_{IO}$) associated with adopting the CSG mesostructure. We suggest this decrease is related to the difference in the d^*_{CSG}/d^*_{LAM} ratios (where $d^* = 2\pi/q^*$) for the two PEO PDI values; this ratio is larger when the PEO PDI = 1.30 than when the PEO PDI = 1 (Table 2). The increase in d^*_{CSG}/d^*_{LAM} means the interfacial area per chain in the CSG mesostructure is lower relative to the LAM_3 morphology for the higher PEO PDI. Consequently, all of the relative segment−segment interaction energies (ΔF_{IS}, ΔF_{SO}, ΔF_{IO}) decrease and thus become more favorable for CSG as the PEO PDI is increased from 1 to 1.30. The net thermodynamic effect is that the interface curves toward the polydisperse terminal PEO blocks, a result consistent with previous AB diblock studies.[8−10,16]

A few other groups hypothesized that polydispersity could be used as a tool to stabilize an ordered network mesostructure. Hasegawa et al. speculated that a distribution of block lengths would help stabilize bicontinuous AB block copolymer mesostructures.[39] Martínez-Veracoechea and Escobedo tested this hypothesis by employing lattice Monte Carlo (MC) simulations to examine bimodal blends of AB diblock copolymers.[40] They found that introducing bidispersity widens the temperature range at which the gyroid is stable in the simulations because the distribution of chain lengths relieves packing frustration, with the longer chains occupying domain centers. They noted that their MC results support the idea that bidispersity could be used to stabilize the gyroid mesostructure. Lynd and Hillmyer reported experimental data that support Martínez-Veracoechea and Escobedo's hypothesis.[10] They identified polydispersity-driven morphological transitions to gyroid at two different compositions in poly((ethylene-*alt*-propylene)-*b*-lactide) diblock copolymers. Schröder-Turk et al. also suggested polydispersity could be used to relieve the packing frustration of complex multiply continuous morphologies.[41] These authors used geometric arguments to suggest that a complex triply continuous phase (called I-WP) could be stabilized in certain multicomponent blends of ABC triblock terpolymers that have varying chain lengths in the C domain and monodisperse A and B domains. None of these previous reports provided experimental evidence that polydispersity could stabilize a network mesostructure in ABC triblock terpolymers. Our experimental results, coupled with the SCFT calculations, show that polydispersity can be used to stabilize the CSG morphology. The network region of the ISO phase diagram has been widened by judicious multicomponent blending,[42] a generic process whose only "cost" is the preparation of additional block terpolymers with different compositions. This result demonstrates that polydispersity is not always undesirable for block copolymers but can be used to tune phase behavior and drive desired morphological transitions.

Acknowledgment. The authors gratefully acknowledge financial support from the Department of Energy through Grant 5-35908 and through a subcontract to UT-Battelle (No. 4000041622). We also acknowledge support from the National Science Foundation (NSF DMR-0220460). Graduate fellowships to A.J.M. from the Department of Homeland Security and the Department of Defense are gratefully acknowledged. Portions of this work were performed at the DuPont−Northwestern−Dow Collaborative Access Team (DND-CAT) located at Sector 5 of the Advanced Photon Source (APS). DND-CAT is supported by E.I. DuPont de Nemours & Co., The Dow Chemical Company, and the State of Illinois. Use of the Advanced Photon Source (APS) was supported by the U.S. Department of Energy, Office of Science, Office of Basic Energy Sciences, under Contract No. DE-AC02-06CH11357. We thank Professor David C. Morse for providing his group's SCFT code and are indebted to Jian Qin for teaching us how to run the code and for many fruitful discussions.

References and Notes

(1) Ruzette, A.; Tence-Girault, S.; Leibler, L.; Chauvin, F.; Bertin, D.; Guerret, O.; Gerard, P. *Macromolecules* **2006**, *39*, 5804–5814.
(2) Bendejacq, D.; Ponsinet, V.; Joanicot, M.; Loo, Y.-L.; Register, R. A. *Macromolecules* **2002**, *35*, 6645–6649.
(3) Matsushita, Y.; Noro, A.; Iinuma, M.; Suzuki, J.; Ohtani, H.; Takano, A. *Macromolecules* **2003**, *36*, 8074–8077.
(4) Noro, A.; Iinuma, M.; Suzuki, J.; Takano, A.; Matsushita, Y. *Macromolecules* **2004**, *37*, 3804–3808.
(5) Noro, A.; Cho, D.; Takano, A.; Matsushita, Y. *Macromolecules* **2005**, *38*, 4371–4376.
(6) Noro, A.; Okuda, M.; Odamaki, F.; Kawaguchi, D.; Torikai, N.; Takano, A.; Matsushita, Y. *Macromolecules* **2006**, *39*, 7654–7661.
(7) Torikai, N.; Noro, A.; Okuda, M.; Odamaki, F.; Kawaguchi, D.; Takano, A.; Matsushita, Y. *Phys. B* **2006**, *385−386*, 709–712.
(8) Sides, S. W.; Fredrickson, G. H. *J. Chem. Phys.* **2004**, *121*, 4974–4986.
(9) Cooke, D. M.; Shi, A. *Macromolecules* **2006**, *39*, 6661–6671.
(10) Lynd, N. A.; Hillmyer, M. A. *Macromolecules* **2005**, *38*, 8803–8810.
(11) Lynd, N. A.; Hillmyer, M. A. *Macromolecules* **2007**, *40*, 8050–8055.
(12) Lynd, N. A.; Hamilton, B. D.; Hillmyer, M. A. *J. Polym. Sci., Part B: Polym. Phys.* **2007**, *45*, 3386–3393.
(13) Lynd, N. A.; Hillmyer, M. A.; Matsen, M. W. *Macromolecules* **2008**, *41*, 4531–4533.
(14) Meuler, A. J.; Ellison, C. J.; Evans, C. M.; Hillmyer, M. A.; Bates, F. S. *Macromolecules* **2007**, *40*, 7072–7074.
(15) Matsen, M. W. *Eur. Phys. J. E* **2007**, *21*, 199–207.
(16) Matsen, M. W. *Phys. Rev. Lett.* **2007**, *99*, 148304.
(17) Lynd, N. A.; Meuler, A. J.; Hillmyer, M. A. Accepted in *Prog. Polym. Sci.*
(18) Milner, S. T.; Witten, T. A.; Cates, M. E. *Macromolecules* **1989**, *22*, 853–861.
(19) Leibler, L. *Prog. Polym. Sci.* **2005**, *30*, 898–914.
(20) Dair, B. J.; Honeker, C. C.; Alward, D. B.; Avgeropoulos, A.; Hadjichristidis, N.; Fetters, L. J.; Capel, M.; Thomas, E. L. *Macromolecules* **1999**, *32*, 8145–8152.
(21) Meuler, A. J.; Fleury, G.; Hillmyer, M. A.; Bates, F. S. *Macromolecules* **2008**, *41*, 5809–5817.
(22) Hashimoto, T.; Tsutsumi, K.; Funaki, Y. *Langmuir* **1997**, *13*, 6869–6872.
(23) Campbell, M.; Sharp, D. N.; Harrison, M. T.; Denning, R. G.; Turberfield, A. J. *Nature (London)* **2000**, *404*, 53–56.
(24) Urbas, A. M.; Maldovan, M.; DeRege, P.; Thomas, E. L. *Adv. Mater.* **2002**, *14*, 1850–1853.
(25) Chan, V. Z.; Hoffman, J.; Lee, V. Y.; Latrou, H.; Avgeropoulos, A.; Hadjichristidis, N.; Miller, R. D. *Science* **1999**, *286*, 1716–1719.
(26) Hillmyer, M. A. *J. Polym. Sci., Part B: Polym. Phys.* **2007**, *45*, 3249–3251.
(27) Bailey, T. S.; Hardy, C. M.; Epps, T. H., III; Bates, F. S. *Macromolecules* **2002**, *35*, 7007–7017.
(28) Hillmyer, M. A.; Bates, F. S. *Macromolecules* **1996**, *29*, 6994–7002.
(29) Rosedale, J. H.; Bates, F. S. *Macromolecules* **1990**, *23*, 2329–2338.
(30) Fetters, L. J.; Lohse, D. J.; Richter, D.; Witten, T. A.; Zirkel, A. *Macromolecules* **1994**, *27*, 4639–4647.
(31) Epps, T. H., III; Cochran, E. W.; Bailey, T. S.; Waletzko, R. S.; Hardy, C. M.; Bates, F. S. *Macromolecules* **2004**, *37*, 8325–8341.
(32) Epps, T. H., III; Cochran, E. W.; Hardy, C. M.; Bailey, T. S.; Waletzko, R. S.; Bates, F. S. *Macromolecules* **2004**, *37*, 7085–7088.
(33) Chatterjee, J.; Jain, S.; Bates, F. S. *Macromolecules* **2007**, *40*, 2882–2896.
(34) Hahn, T., Ed. *International Tables for Crystallography*, 4th revised ed.; **1994**; Vol. *A*.
(35) Tyler, C. A.; Morse, D. C. *Phys. Rev. Lett.* **2005**, *94*, 208302.
(36) Tyler, C. A.; Qin, J.; Bates, F. S.; Morse, D. C. *Macromolecules* **2007**, *40*, 4654–4668.
(37) Miao, B.; Wickham, R. A. *J. Chem. Phys.* **2008**, *128*, 054902.
(38) Nguyen, D.; Zhong, X.; Williams, C. E.; Eisenberg, A. *Macromolecules* **1994**, *27*, 5173–5181.
(39) Hasegawa, H.; Hashimoto, T.; Hyde, S. T. *Polymer* **1996**, *37*, 3825–3833.
(40) Martínez-Veracoechea, F. J.; Escobedo, F. A. *Macromolecules* **2005**, *38*, 8522–8531.
(41) Schröder-Turk; G. E.; Fogden, A.; Hyde, S. T. *Eur. Phys. J. B* **2007**, *59*, 115–126.
(42) The CSG morphology was identified in two other multicomponent ISO blends with overall $f_O = 0.33$. These blends were comprised of samples from the series of ISO triblocks used to prepare ISO(0.33, 1.30) but had different PEO PDI values. The complete details of the phase behavior of these samples will be included in a forthcoming publication.

MA8010894